A new family of Polak-Ribière-Polyak conjugate gradient method for impulse noise removal

Ali Mousavi
Islamic Azad University Sanandaj Branch
Mansour Esmaeilpour (ma.esmaeilpour@gmail.com)
IAU: Islamic Azad University https://orcid.org/0000-0002-2475-518X
Amir Sheikhahmadi
Islamic Azad University Sanandaj Branch

Research Article

Keywords: Image Processing, Impulse Noise Removal, Convex optimization, Conjugate gradient approach.

Posted Date: May 2nd, 2023

DOI: https://doi.org/10.21203/rs.3.rs-2455051/v1

Version of Record: A version of this preprint was published at Soft Computing on September 28th, 2023.
See the published version at https://doi.org/10.1007/s00500-023-09232-3.

A new family of Polak-Ribière-Polyak conjugate gradient method for impulse noise removal

Ali Mousavi[a], **Mansour Esmaeilpour**[b], **Amir Sheikhahmadi**[a]

Received: date / Accepted: date

Abstract In this paper, impulse noise removal problem is formulated as an unconstrained optimization problem with smooth objective function. It can be solved by conjugate gradient methods with desired properties (low memory and strong global convergence) in high dimensions. Accordingly, a family of the Polak-Ribière-Polyak (PRP) conjugate gradient directions is constructed for which the descent condition holds. In other words, we introduce four improved versions of PRP method three of which are based on a regularization and one of which is the combination of Fletcher-Reeves and PRP conjugate gradient parameters. Using several images, it is shown that the new methods are very robust and efficient in comparison with other competitive methods for impulse noise removal, especially in terms of the peak signal to noise ratio (PSNR).

Keywords Image Processing · Impulse Noise Removal · Convex optimization · Conjugate gradient approach.

Mathematics Subject Classification (2000) 90C30a · 90C25 · 90C90 · 68U10 · 03D15

1 Introduction

The problem of impulse noise removal from images has been investigated by many researchers for many years [1–4, 10–14, 16, 20, 25]. Due to the variation in noises, impulse noise removal methods are also different. They have two important properties: (1) The noise reduction rate from the corrupted images. (2) The speed of the algorithm implementation. Removing a noise from medical images is very important in the medical science. Images with high resolution helps to diagnose diseases and also speeds up the treatment process. There are various noises in medical images such as Gaussian noise, Rayleigh noise and Poisson noise [12, 20, 25]. Impulse noise often appears in acquisition, transmission, storage, and processing of medical reduce the image quality and to eliminate many of the details in the image. There are many ways to remove images. Impulse noises in medical image cause to impulse noise such as median filter [1], wavelet filter [12], fuzzy algorithms [16, 20], and optimization method [15].

Most of available methods are made on the basis of median filter methods, which use the information of the noisy pixels. The standard median filter removes the noisy pixels by replacing test pixel with the median value of the noisy pixels. For images with the small noise, this method is very effective but the results are not good for images with high-level of noise, cf. [1].

In 2007, two-step algorithms have been suggested to remove impulse noise [2, 10]. In the first step, the noisy pixels are identified by the median filter method. In the second step, these noises are removed by solving an unconstrained optimization problem. Let x be the original image contain $M \times N$ pixels. The index set of original image x is defined by

$$A = \{(i, j) \,|\, i = 1, 2, \cdots, M,\ j = 1, 2, \cdots, N\}.$$

Corresponding author: Mansour Esmaeilpour
Email: esmaeilpour@iauh.ac.ir
[a] Department of Computer Engineering, Sanandaj Branch, Islamic Azad University, Sanandaj, Iran
[b] Computer Engineering Department, Hamedan Branch, Islamic Azad University, Hamedan, Iran

In addition, y and $\tilde{y}$ are the image with salt and pepper impulse noise and the image obtained by applying median filter method, respectively. We now require to modify the pixel $x_{i,j}$ while $\tilde{y}_{i,j}$ are the recovered pixels by the median filter method. Consider the four closest neighborhoods of $x_{i,j}$ as $x_{i-1,j}$, $x_{i,j-1}$, $x_{i,j+1}$ and $x_{i+1,j}$ denoted by $V_{i,j}$.

	$x_{i-1,j}$	
$x_{i,j-1}$	$x_{i,j}$	$x_{i,j+1}$
	$x_{i+1,j}$	

Using the median filter method, we express the noisy pixels as $s_{\min}$, $s_{\max}$ and $x_{i,j}$ with $0 \leq p \leq 1$, $0 \leq q \leq 1$ and $1-p-q$ probability, respectively. Note that $[s_{\min}, s_{\max}]$ is dynamic range of original image [1].

We define the following set of indices

$$N = \{(i,j) \in A \mid \tilde{y}_{i,j} \neq y_{i,j}, \quad y_{i,j} = s_{\min} \text{ or } s_{\max}\},$$

and its complement by

$$N^C = \{(i,j) \in A \mid (i,j) \notin N\}.$$

Therefore, in the first step, the median filter method detects the noisy pixels. Let $(i,j) \in N$. In other words, $x_{i,j}$ is noisy pixel, $c = |N|$, and

$$u = \Big[u_{i,j}\Big]_{(i,j)\in N} \in \mathbb{R}^c,$$

is the vector containing all noisy pixels. Let us denote an edge-preserving function by φ_ω and

$$S^1_{i,j} = \sum_{(m,n)\in V_{i,j}\setminus N} \varphi_\omega(u_{i,j} - y_{m,n}),$$
$$S^2_{i,j} = \sum_{(m,n)\in V_{i,j}\bigcap N} \varphi_\omega(u_{i,j} - u_{m,n}).$$

As in [2,4,15,21], the goal is to solve the unconstrained optimization problem with non-smooth objective function for impulse noise removal in the second step

$$\min_{u\in\mathbb{R}^c} \psi_\omega(u) := \sum_{(i,j)\in N} |u_{i,j} - y_{i,j}| + \frac{\eta}{2} \sum_{(i,j)\in N} (2S^1_{i,j} + S^2_{i,j}),$$

where $\eta > 0$ is regularization parameter. The edge-preserving function needs to assume the following

1) φ_ω is twice continuously differentiable,
2) $\varphi''_\omega > 0$,
3) φ_ω is even function.

A very common example of this function is $\varphi_\omega(u) = \sqrt{u^2 + \omega}$ where $\omega > 0$ is a arbitrary parameter. The first term in $\psi_\omega(u)$ is not smooth. Hence, we eliminate the non-smooth part of $\psi_\omega(u)$ and obtain a smooth function. In other words, we are interested in minimizing the following objective function in the second step

$$F_\omega(u) = \eta \sum_{(i,j)\in N} \Big(S^1_{i,j} + \frac{1}{2} S^2_{i,j}\Big).$$

where both $S^1_{i,j}$ and $S^2_{i,j}$ were defined earlier. There are many optimization methods to solve this unconstrained problem. Generally, optimization methods solve unconstrained optimization problems

$$\min_{x\in\mathbb{R}^c} F_\omega(u), \tag{1}$$

in which $F_\omega : \mathbb{R}^c \longrightarrow \mathbb{R}$, starting from the initial point $u_0 \in \mathbb{R}^c$ and obtaining the sequence $\{u_k\}$

$$u_{k+1} = u_k + \alpha_k d_k, \qquad k = 0, 1, 2, ...$$

Here α_k is the step-size and d_k is a descent direction; i.e., $g_k^T d_k < 0$ for all $k \geq 0$ where $g_k = \nabla F_\omega(u_k)$.

2 Conjugate gradient methods

Conjugate gradient method is one of effective iterative methods to solve the unconstrained optimization problems whose objective function is a smooth. There are two main reasons why these methods are efficient for solving unconstrained optimization problems: low memory requirement and strong local and global convergence properties. In addition, they do not require any matrix storage and are suitable to solve large-scale optimization problems, see [8,17,22,23].

In conjugate gradient methods, the direction d_k is computed by

$$d_k = \begin{cases} -g_k, & k = 0, \\ -g_k + \beta_k d_{k-1}, & k \geq 1, \end{cases}$$

where β_k is called the conjugate gradient parameter. However, different selections for this parameter lead to various conjugate gradient methods, some of which are

$$\beta_k^{HS} = \frac{g_k^T y_{k-1}}{d_{k-1}^T y_{k-1}}, \qquad \text{(Hestenes-Stiefel)([9])}$$

$$\beta_k^{FR} = \frac{\|g_k\|^2}{\|g_{k-1}\|^2}, \qquad \text{(Fletcher-Reeves)([7])}$$

$$\beta_k^{DY} = \frac{\|g_k\|^2}{d_{k-1}^T y_{k-1}}, \qquad \text{(Dai-Yuan)([5])}$$

$$\beta_k^{HZ} = \beta_k^{HS} - 2\|y_{k-1}\|^2 \frac{g_k^T d_{k-1}}{(d_{k-1}^T y_{k-1})^2}, \qquad \text{(Hager-Zhang)([8])}$$

$$\beta_k^{PRP} = \frac{g_k^T y_{k-1}}{\|g_{k-1}\|^2}, \qquad \text{(Polak-Ribière-Polyak)([18,19])}$$

in which $y_{k-1} = g_k - g_{k-1}$ and $\|\cdot\|$ denotes the Euclidean norm. After computing the descent direction, we compute the step-size by solving an one-dimensional optimization problem. Usually, the step-size is inexact and satisfies either Armijo, Wolfe, or Goldstein conditions [17].

3 Contribution and organization

In this paper, we use two-step algorithm for impulse noise removal. The first step is to use an adaptive median filter to recovery a noisy image. The second step is a new regularized conjugate gradient based on Polak-Ribière-Polyak method. Four improved versions of Polak-Ribière-Polyak method are introduced, three of which are based on a regularization and one of which preserves advantages the FR and PRP conjugate gradient parameters. We prove the descent property of the new directions. The global convergence of our method can be done in the same way as [24]. The numerical results show that the new methods are able to eliminate noise from images, confirming the fact that our new methods are effective and robust for impulse noise removal.

In Section 4, we describe our proposed method for impulse noise removal. The descent property and the global convergence of the new method are established in Section 5. In Section 6, some numerical results are given showing the fact that our new method is competitive. Finally, some conclusions are summarized in Section 7.

4 New method

One of the well-known conjugate gradient method to solve unconstrained optimization problems is the Polak-Ribière-Polyak method which introduced in 1969 [18,19]. Although the convergence properties of this method is not strong for some functions, its numerically performance is good. To improve the efficiency of this method for impulse noise removal, we modify the Polak-Ribière-Polyak conjugate gradient method. To simplify our notation, we denote $F(u) := F_\omega(u)$.

Our method wants to solve the unconstrained optimization problem (1) by starting from the initial point $u_0 \in \mathbb{R}^c$ and by generating $u_{k+1} = u_k + \alpha_k d_k^{PRP}$ with $d_0^{PRP} = -\nabla F_0$, $d_k^{PRP} =$

$-\nabla F_k + \beta_k^{PRP} d_{k-1}^{PRP}$, $\beta_k^{PRP} = \dfrac{\nabla F_k^T y_{k-1}}{\|\nabla F_{k-1}\|^2}$, $\nabla F_k = \nabla F(u_k)$ and $y_{k-1} = \nabla F_k - \nabla F_{k-1}$. Moreover, the step-size α_k satisfies in the following strong Wolfe condition [17]

$$\begin{cases} F_{k+1} < F_k + c_1 \nabla F_k^T d_k^{PRP}, \\ |\nabla F_{k+1}^T d_k^{PRP}| < -c_2 \nabla F_k^T d_k^{PRP}, \end{cases}$$

where $0 < c_1 < c_2 < 1$. We now suggest the following four versions of our new methods which are obtained by modifying the Polak-Ribière-Polyak method:

(1) **NPRP1** using

$$d_k^{NPRP1} = -\nabla F_k + \frac{\beta_k^{PRP}}{y_{k-1}^T d_{k-1}^{NPRP1} + \|y_{k-1}\| \|d_{k-1}^{NPRP1}\|} d_{k-1}^{NPRP1}.$$

(2) **NPRP2** using

$$d_k^{NPRP2} = -\nabla F_k + \frac{\beta_k^{PRP}}{\nabla F_k^T d_{k-1}^{NPRP2} + \|\nabla F_k\| \|d_{k-1}^{NPRP2}\|} d_{k-1}^{NPRP2}.$$

(3) **NPRP3** using

$$d_k^{NPRP3} = -\nabla F_k + \frac{\beta_k^{PRP}}{\nabla F_k^T \nabla F_{k-1} + \|\nabla F_k\| \|\nabla F_{k-1}\|} d_{k-1}^{NPRP3}.$$

(4) **NPRP4.** In this method, we consider three following cases.

Case 1. If $(\nabla F_k^T y_{k-1})(\nabla F_k^T d_{k-1}^{NPRP4}) < 0$ then

$$d_k^{NPRP4} = -\theta_k \nabla F_k + \beta_k^{PRP} d_{k-1}^{NPRP4}.$$

Case 2. For $\nabla F_k^T d_{k-1}^{NPRP4} > 0$, we use

$$d_k^{NPRP4} = -\theta_k \nabla F_k - \beta_k^{FR} d_{k-1}^{NPRP4},$$

Case 3. If case (1) and case (2) are not hold, we have

$$d_k^{NPRP4} = -\theta_k \nabla F_k,$$

We define the new parameter θ_k as follows

$$\theta_k = \frac{\|y_{k-1}\|^2}{\|s_{k-1}\|^2},$$

and $s_{k-1} = u_k - u_{k-1}$.

NPRP1-NPRP3 use a regularization technique which is useful in the presence of rounding errors. Besides, NPRP4 is a combination of FR and PRP conjugate gradient parameters and the new step size θ_k, defined above.

5 Convergence analysis

In this section, we prove the descent condition for generated directions by NPRP4. To this goal, we consider the following assumptions:

(H1) For any $u_0 \in \mathbb{R}^c$, the level set

$$L(u_0) = \{u \in \mathbb{R}^c | F_\omega(u) \leq F_\omega(u_0)\},$$

is bounded.

(H2) The gradient of $F_\omega(u)$ is Lipschitz continuous, i.e., there exists constant $L > 0$ such that

$$\|\nabla F_\omega(u) - \nabla F_\omega(v)\| \leq L\|u - v\|,$$

for any $u, v \in L(u_0)$.

(H3) The function $F_\omega(u)$ is uniformly convex, i.e., there exists constant $\gamma > 0$ such that

$$\gamma\|u - v\|^2 \leq \Big(\nabla F_\omega(u) - \nabla F_\omega(v)\Big)^T (u - v),$$

for any $u, v \in L(u_0)$.

Theorem 1 *The direction d_k^{NPRP4} is a descent direction, i.e.,*

$$\nabla F_k^T d_k^{NPRP4} < 0.$$

Proof We prove that the descent condition of generated directions by NPRP4 holds. To do so, we consider the following three cases:
Case 1. If $(\nabla F_k^T y_{k-1})(\nabla F_k^T d_{k-1}^{NPRP4}) < 0$, then

$$\begin{aligned}\nabla F_k^T d_k^{NPRP4} &= -\theta_k \|\nabla F_k\|^2 + \beta_k^{PRP} \nabla F_k^T d_{k-1}^{NPRP4} \\ &= -\theta_k \|\nabla F_k\|^2 + \frac{\nabla F_k^T y_{k-1}}{\|\nabla F_{k-1}\|^2} \nabla F_k^T d_{k-1}^{NPRP4} < 0.\end{aligned}$$

Case 2. If $\nabla F_k^T d_{k-1}^{NPRP4} > 0$, then

$$\begin{aligned}\nabla F_k^T d_k^{NPRP4} &= -\theta_k \|\nabla F_k\|^2 - \beta_k^{FR} \nabla F_k^T d_{k-1}^{NPRP4} \\ &= -\theta_k \|\nabla F_k\|^2 - \frac{\|\nabla F_k\|^2}{\|\nabla F_{k-1}\|^2} \nabla F_k^T d_{k-1}^{NPRP4} < 0.\end{aligned}$$

Case 3. In this case, we use the steepest descent direction, so that

$$\nabla F_k^T d_k^{NPRP4} = -\theta_k \|\nabla F_k\|^2 < 0.$$

Therefore, in all cases the direction d_k^{NPRP4} is a descent direction. □

Now, the global convergence of the NPRP4 method is proven in the following theorem.

Theorem 2 *Let **(H1)-(H3)** hold. Then, the NPRP4 method converges to the optimal solution of the unconstrained optimization problem.*

Proof The new method (NPRP4) for impulse noise removal is based on PRP and FR methods which their convergence analysis is stablished in [24]. Therefore, we conclude that the NPRP4 is globally convergent.

6 Numerical results

In this section, to demonstrate the efficiency of the NPRP4 method to remove noise from medical images, we compare obtained numerical results of our method with other three new methods and some conjugate gradient methods, discussed in Section 2. To evaluate the amount of images restoration, we use the peak signal to noise ratio (PSNR) which is defined as [2]

$$PSNR = 10 \log_{10} \frac{255^2}{\frac{1}{MN} \sum_{i,j} (u_{i,j}^r - u_{i,j}^*)^2},$$

in which $u_{i,j}^*$ and $u_{i,j}^r$ are the pixel values of the original image and the restored image, respectively. The condition of stopping all algorithms are

$$\frac{|F_\omega(u_k) - F_\omega(u_{k-1})|}{|F_\omega(u_k)|} < 10^{-4},$$

and

$$\frac{\|\alpha_k d_k\|}{\|u_k\|} \leq 10^{-4}.$$

The parameters used in all algorithms are $\omega = 10^{-4}$, $c_1 = 10^{-4}$ and $c_2 = 0.5$. All algorithms are implemented in Matlab 2011 on a laptop with a 2.5 GHz Intel Core i5-3210M CPU and 4 GB of memory. The test images are 256×256 Lena, 256×256 House, 256×256 Cameraman, 512×512 Cameraman, 512×512 HeadCT, and 512×512 CerebSagE. These images are available on the following websites:

- http://www.imageprocessingplace.com/root_files_V3/image_databases.htm
- https://homepages.cae.wisc.edu/ece533/images/

To compare all solvers and identify the best solver, four cost measures the average of total number of iterations (N_i), the average of function evaluations (N_f) , times in second (C_t) and PSNR are used. Let S be the list of all compared solvers and let P be the list of all test images. All solvers are performed to recover all test corrupted images and the obtained results are summarized in Tables 1-4. Let us call the performance profile by Dolan and Morè [6] to plot Figures 1-6 in terms of PSNR which is an important cost measure. We describe how this performance profile works. It takes lists S, P and the PSNR matrix. It uses the performance rate

$$r_{p,s} = \frac{t_{p,s}}{\min\{t_{p,s} \,|\, s \in S\}},$$

to compute the strength of a solver $s \in S$ by

$$\rho_s(z) = \frac{1}{n_p}\Big|\{p \in P \,|\, r_{p,s} \leq z\}\Big|,$$

in which $z \in \mathbb{R}$ and $\rho_s(z)$ is the cumulative distribution function.

As can be seen in Figures 1-4, NPRP1-NPRP4 are more efficient than the traditional PRP in terms of PSNR. From Figure 5, we conclude that NPRP4 is very competitive version of our methods in terms of PSNR. Figure 6 shows other known conjugate gradient solvers.

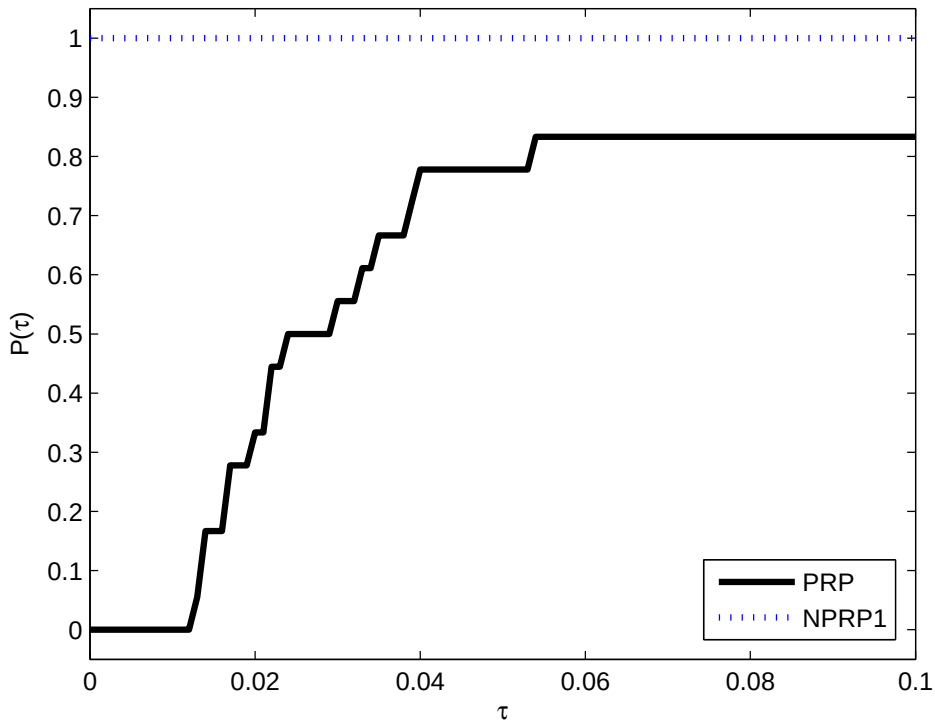

Fig. 1 Performance profile for PRP and NPRP1 in terms of PSNR

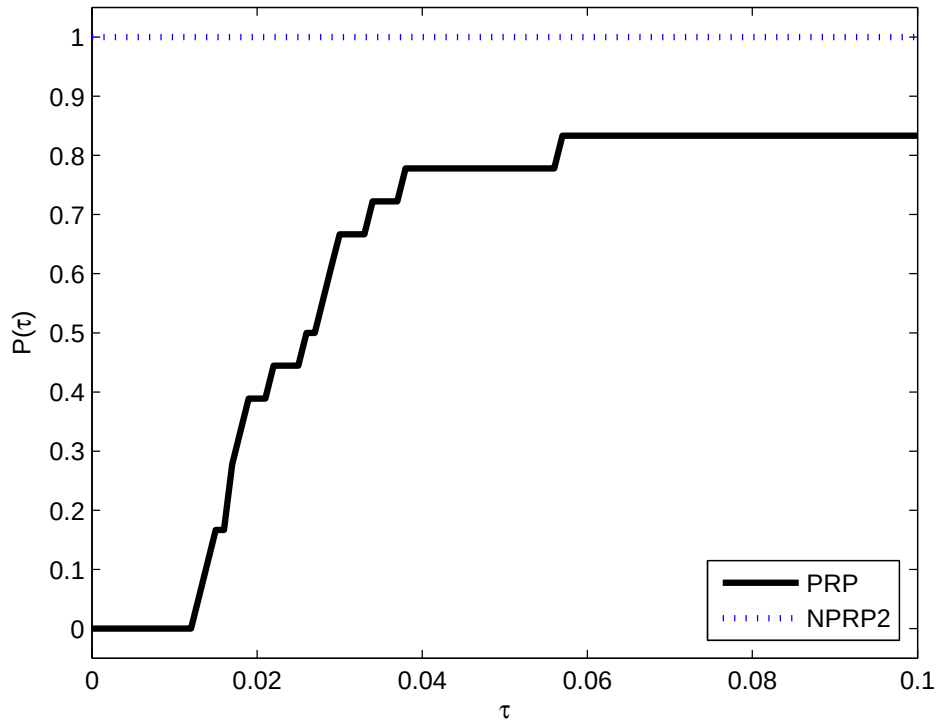

Fig. 2 Performance profile for PRP and NPRP2 in terms of PSNR

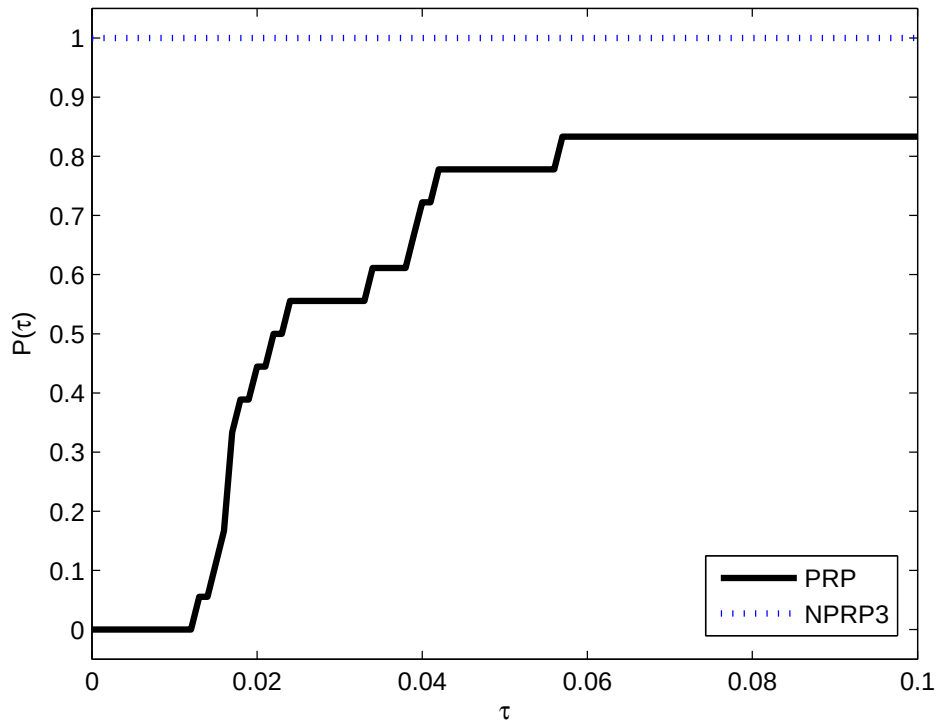

Fig. 3 Performance profile for PRP and NPRP3 in terms of PSNR

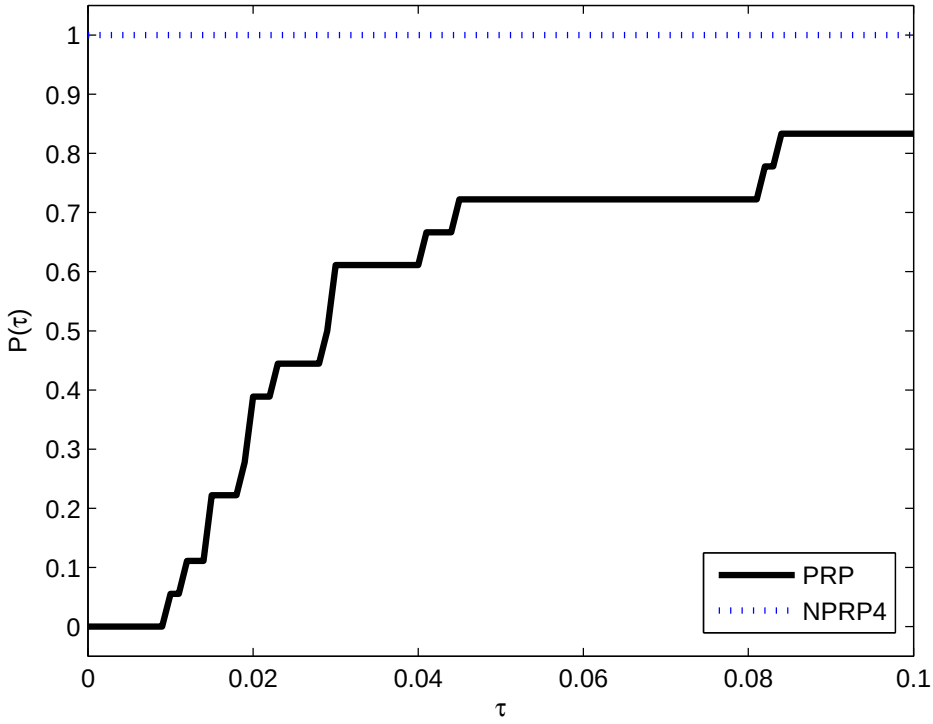

Fig. 4 Performance profile for PRP and NPRP4 in terms of PSNR

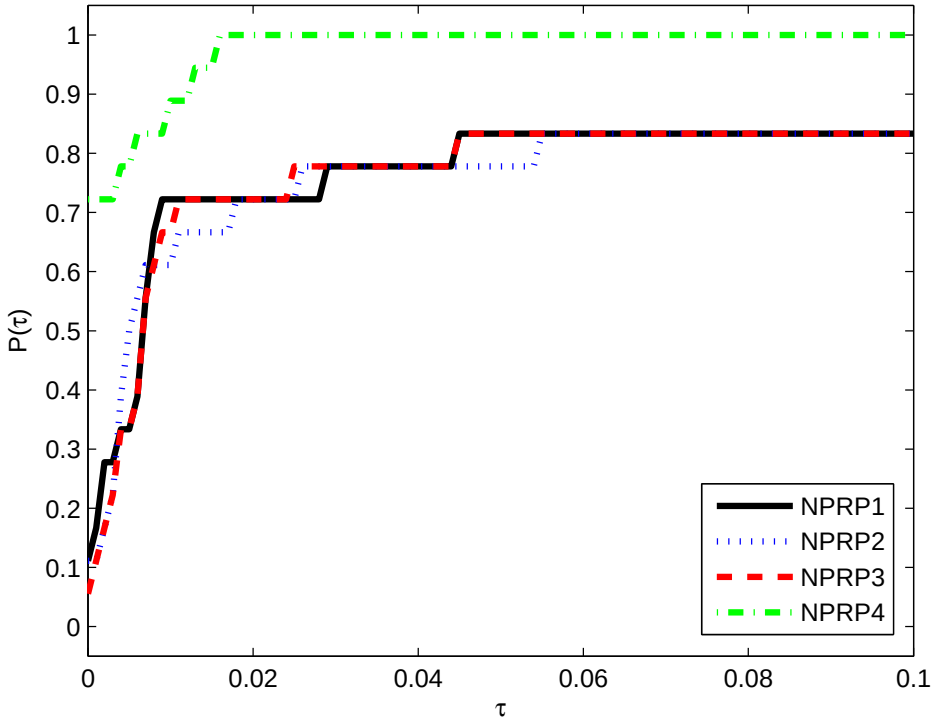

Fig. 5 Performance profile for NPRP1, NPRP2, NPRP3 and NPRP4 in terms of PSNR

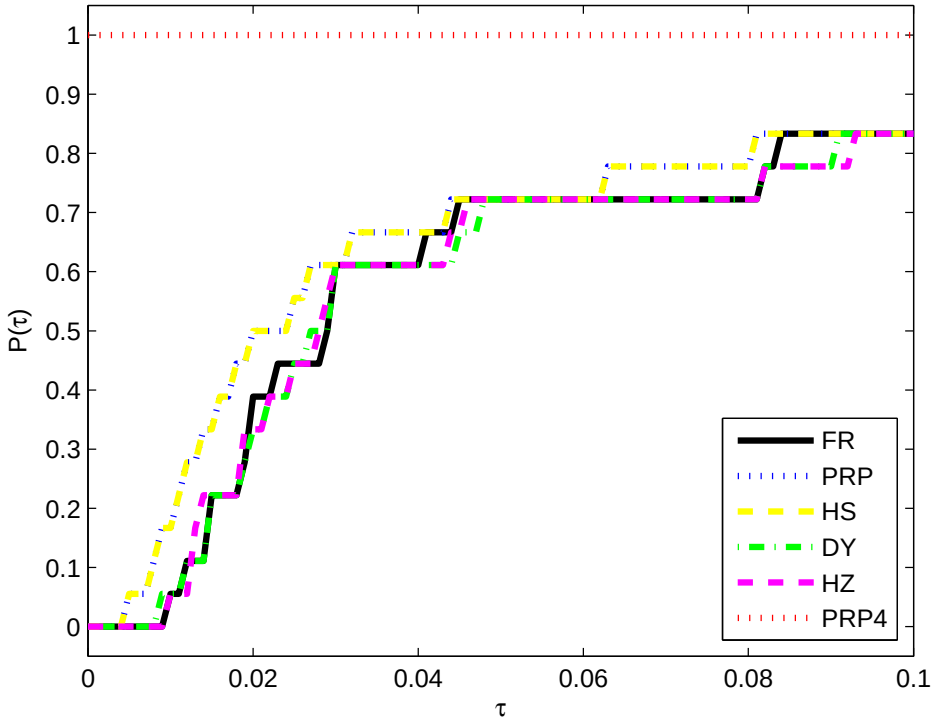

Fig. 6 Performance profile for FR, PRP, HS, DY, HZ and NPRP4 in terms of PSNR

7 Concluding remarks

In this paper, based on PRP method, a new conjugate gradient method introduced to solve smooth unconstrained problem to remove impulse noise from medical images. The generated directions satisfied the descent condition. Several standard images used to show the robust and efficient the new method in comparison with other competitive methods for impulse noise removal.

Compliance with ethical standards

Ethical approval This article does not contain any studies with human participants or animals performed by any of the authors.
Conflict of interest All authors declare that they have no conflict of interest.
Funding details No funds have been used.
Author contributions All authors participated equally in the preparation of the article.

References

1. M. Abreu, M. Lightstone, S. K. Mitra, K. Arakawa, *A new efficient approach for the removal of impulse noise from highly corrupted images*, IEEE Trans. Image. Process, **5(11)**, 11-15 (1991).
2. J. F. Cai, R. H. Chan, B. Morini, *Minimization of an edge-preserving regularization functional by conjugate gradient type methods, image processing based on partial differential equations*, In Mathematics and Visualization, Springer, Berlin Heidelberg, 901-911, (2007), DOI:10.1007/s10851-007-0027-4.
3. R. Chan, C. Hu, M. Nikolova, *Iterative procedure for removing random-valued impulse noise*, IEEE Signal Process. Lett, **11(12)**, 921-924 (2004).
4. T. F. Chan, J. Shen, H. Zhou, *Total variation wavelet inpainting*, J. Math. Imaging Vision, **25**, 107-125 (2006).
5. Y. H. Dai, Y. Yuan, *A nonlinear conjugate gradient method with a strong global convergence property*, IEEE SIAM J. Optim, **10**, 177-182 (1999).
6. E. Dolan, J. J. Morè, *Benchmarking optimization software with performance profiles*, Math. Program, **19(2)**, 201-213, (2002).

7. R. Fletcher, C. Reeves, *Function minimization by conjugate gradients*, Compu. J., **7**, 149-154 (1964).
8. W. W. Hager, H. Zhang, *A survey of nonlinear conjugate gradeint methods*, (2005), http://www.math.u.edu/hager.
9. M. R. Hestenes, E. L. Stiefel, *Methods of conjugate gradients for solving linear systems*, J. Research Nat. Bur. Standards, **49**, 409-436 (1952).
10. D. Hongyao, Z. Qingxin, S. Xiuli, J. Tao, *A decision-based modified total variation diffusion method for impulse noise removal*, Computational Intelligence and Neuroscience, vol. 2017, Article ID 2024396, 20 pages.
11. L. Jin, W. Zhang, G. Ma, E. Song, *Learning deep CNNs for impulse noise removal in images*, Journal of Visual Communication and Image Representation, **62**, 193-205 (2019).
12. K. Karthikeyan, C. Chandrasekar, *Speckle Noise Reduction of Medical Ultrasound Images using Bayesshrink Wavelet Threshold*, International Journal of Computer Applications, **22(9)**, 8-14 (2011).
13. M. Kimiaei, F. Rahpeymaii, *Impulse noise removal by an adaptive trust-region method*, Soft Computing, **23**, 11901-11923 (2019).
14. M. Kimiaei, M. Rostami, *Impulse noise removal based on new hybrid spectral conjugate gradient approach*, KYBERNETIKA, **52(5)**, 791-823 (2016).
15. J. Liu, S. Li, *Spectral gradient method for impulse noise removal*, Optimization Letters, **9**, 1341-1351 (2015).
16. M. Nadeem, A. Hussain, A. Munir, M. Habib, M. T. Naseem, *Removal of Random Valued Impulse Noise from Grayscale images using Quadrant based Spatially Adaptive Fuzzy Filter*, Signal Processing, **169**, (2020), https://doi.org/101016/j.sigpro.2019107403.
17. J. Nocedal, S. I. Wright, *Numerical Optimization*, Springer, New York, (2006).
18. E. Polyak, G. Ribière, *Note sur la convergence de directions conjugees*, Francaise Informat Recherche Opertionelle, 3e Annee, **16**, 35-43 (1969).
19. B. T. Polyak, *The conjugate gradient method in extreme problems*, USSR Comp. Math. Math. Phys., **9**, 94–112 (1969).
20. F. Russo, G. Ramponi, *A fuzzy filter for images corrupted by impulse noise*, IEEE Signal Processing Letters, **3**, 168-170 (2020).
21. M. Sindhana Devi, M. Soranamageswari, *Efficient impulse noise removal using hybrid neuro fuzzy filter with optimized intelligent water drop technique*, Imaging systems and technology, **29(4)**, 465-475 (2019).
22. G. Yuan, T. Li, W. Hu. *A conjugate gradient algorithm and its application in large-scale optimization problems and image restoration*, Journal of Inequalities and Applications, **247**, (2019).
23. G. Yuan, X. Wang, Z. Sheng, *The projection technique for two open problems of unconstrained optimization problems*, Journal of Optimization Theory and Applications, **186** 590-619, (2020).
24. Y. Wang, C. Yang, A. G. Yagola, *Optimization and regularization for computational inverse problems and applications*, Springer (2011).
25. W. Zhang, L. Jin, E. Song, X. Xu, *Removal of impulse noise in color images based on convolutional neural network*, Applied Soft Computing, **82** (2019), https://doi.org/101016/j.asoc.2019105558.

Table 1 The total number of iterations for recovering the noisy images

Image	Size	Solver								
		FR	PRP	HS	DY	HZ	NPRP1	NPRP2	NPRP3	NPRP4
Lena	$256 * 256$	87	46.67	38.67	89.33	65	47.33	48.67	53.67	29
House	$256 * 256$	60.33	31.33	31.67	59	57	36	41	35.67	22
Cameraman	$256 * 256$	122	47	48	128.67	85	54	54.33	62	32
Cameraman	$512 * 512$	59.33	37.67	33	57.33	49.33	39.67	42	39	22
HeadCT	$512 * 512$	2415.7	184.33	252.67	1900.7	1010.3	303.67	308.33	303.33	40.33
CerebSagE	$512 * 512$	184	45	49	280	244.33	74.67	65.33	65.67	26.33
Avarage		488.06	65.33	75.50	419.17	251.83	92.56	93.28	93.22	28.61

Table 2 The total number of function evaluations for recovering the noisy images

Image	Size	Solver								
		FR	PRP	HS	DY	HZ	NPRP1	NPRP2	NPRP3	NPRP4
Lena	$256 * 256$	357.67	298.67	248.67	368	358	286.33	296	325.33	250.33
House	$256 * 256$	284.67	199.33	203.33	287.33	290.33	214	246.67	212.33	182.67
Cameraman	$256 * 256$	391.33	299.67	310.67	394.33	436	324.33	327.67	373.67	259.33
Cameraman	$512 * 512$	266.67	242	213	272	264.33	237.33	252	233.33	179.67
HeadCT	$512 * 512$	4073	1193.3	1661.3	3908.3	5062.3	1759.3	1792.3	1757	352.67
CerebSagE	$512 * 512$	751	288	316.67	1338.3	1239.7	441	384.67	386.67	223.67
Avarage		1020.7	420.16	492.27	1094.71	1275.11	543.18	549.89	548.06	241.39

Table 3 The CPU times for recovering the noisy images

Image	Size	Solver								
		FR	PRP	HS	DY	HZ	NPRP1	NPRP2	NPRP3	NPRP4
Lena	$256 * 256$	10.04	8.14	6.61	10.15	10.06	7.48	7.57	8.32	6.72
House	$256 * 256$	7.74	5.04	5.40	7.70	7.80	5.54	6.23	5.49	4.69
Cameraman	$256 * 256$	10.94	8.18	8.43	11.14	12.03	8.69	8.70	9.76	6.83
Cameraman	$512 * 512$	46.84	42.31	37.32	47.78	46.48	41.60	43.95	40.88	31.81
HeadCT	$512 * 512$	687.76	198.66	279.08	666.74	752.87	295.45	301.33	294.95	58.72
CerebSagE	$512 * 512$	128.94	49.14	58.82	227.73	210.04	74.53	64.97	65.35	38.25
Avarage		148.71	51.91	65.94	161.87	189.88	72.22	72.13	70.79	24.50

Table 4 The PSNR for recovering the noisy images

Image	Size	Solver								
		FR	PRP	HS	DY	HZ	NPRP1	NPRP2	NPRP3	NPRP4
Lena	$256 * 256$	26.87	26.90	26.93	26.87	26.86	27.22	27.17	27.15	27.11
House	$256 * 256$	30.30	30.43	30.36	30.29	30.29	30.73	30.68	30.76	30.82
Cameraman	$256 * 256$	24.49	24.54	24.52	24.49	24.47	24.86	24.83	24.81	24.94
Cameraman	$512 * 512$	30.18	30.26	30.27	30.20	30.21	30.70	30.70	30.71	30.94
HeadCT	$512 * 512$	8.20	13.85	12.68	8.15	8.06	17.23	17.16	17.20	20.50
CerebSagE	$512 * 512$	28.52	28.85	28.83	28.44	28.46	29.29	29.35	29.38	29.46
Avarage		24.76	25.81	25.60	24.74	24.73	26.67	26.65	26.67	27.30

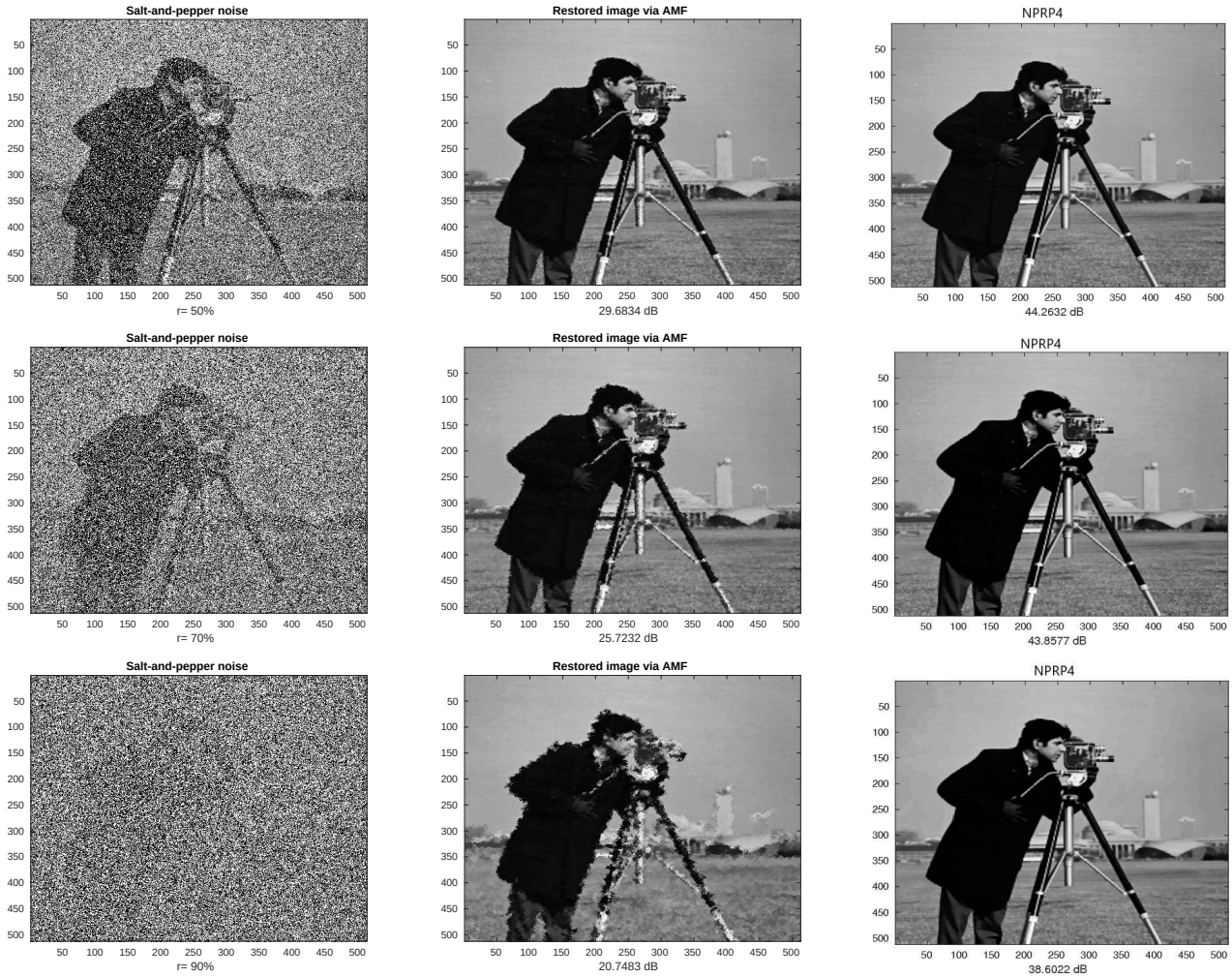

Fig. 7 The noisy images with 50%, 70% and 90% of noises \ the restored images via median filter (AMF) \ the restored images via NPRP4 for Cameraman_256 image.

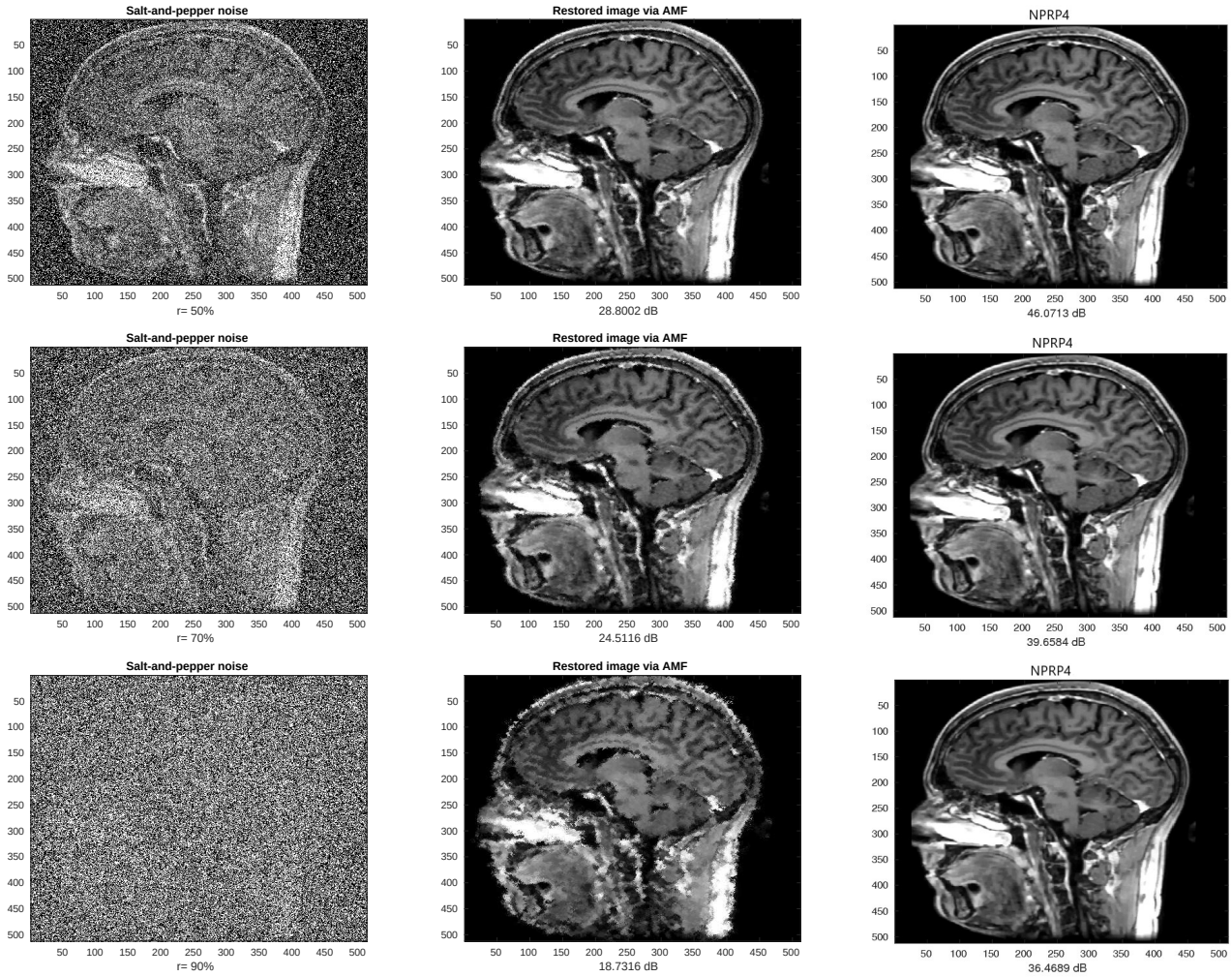

Fig. 8 The noisy images with 50%, 70% and 90% of noises \ the restored images via median filter (AMF) \ the restored images via NPRP4 for HeadCT image.

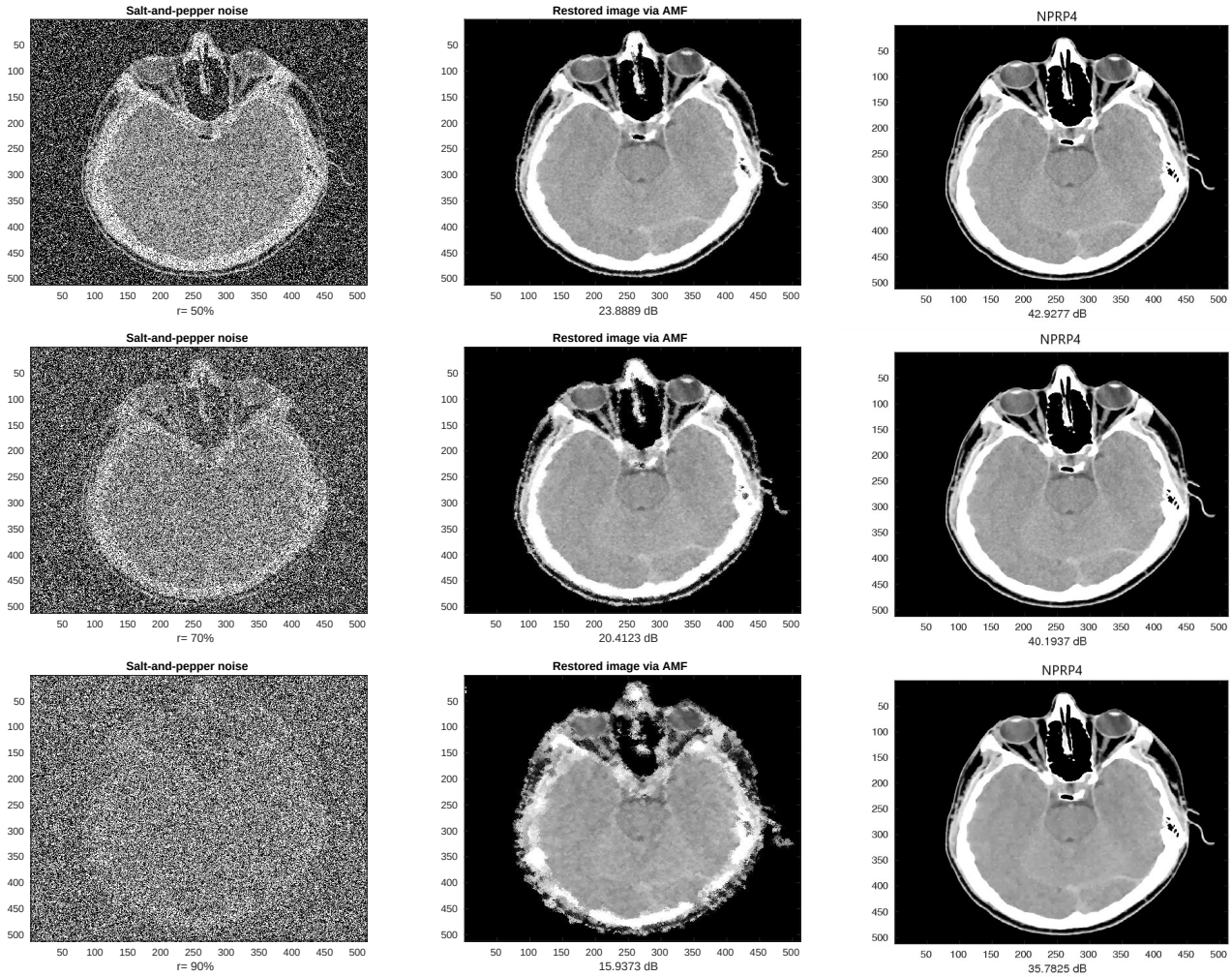

Fig. 9 The noisy images with 50%, 70% and 90% of noises \ the restored images via median filter (AMF) \ the restored images via NPRP4 for CerebSagE image.